Molecular Pharmacology Fast Forward. Published on August 27, 2019 as DOI: 10.1124/mol.119.117333
This article has not been copyedited and formatted. The final version may differ from this version.

Title Page

Title

CYP3A4 induction in the liver and intestine of PXR/CYP3A-humanized mice: approaches by mass spectrometry imaging and portal blood analysis

Names of authors

Kaoru Kobayashi, Jiro Kuze, Satoshi Abe, Shoko Takehara, Genki Minegishi, Katsuhide Igarashi, Satoshi Kitajima, Jun Kanno, Takushi Yamamoto, Mitsuo Oshimura, Yasuhiro Kazuki

Affiliations of authors

Laboratory of DDS Design and Drug Disposition, Graduate School of Pharmaceutical Sciences, Chiba University, Chiba, Japan (K.K., G.M.); Discovery Drug Metabolism & Pharmacokinetics, Tsukuba Research Center, Taiho Pharmaceutical Co., Ltd., Ibaraki, Japan (J.K.); Chromosome Engineering Research Center (CERC), Tottori University, Tottori, Japan (S.A., S.T., M.O., Y.K.); Laboratory of Biofunctional Science, Hoshi University, School of

Molecular Pharmacology Fast Forward. Published on August 27, 2019 as DOI: 10.1124/mol.119.117333
This article has not been copyedited and formatted. The final version may differ from this version.

Pharmacy and Pharmaceutical Sciences (K.I.); Division of Cellular and Molecular Toxicology, Biological Safety Research Center, National Institute of Health Sciences, Kanagawa, Japan (S.K., J.K.); Japan Bioassay Research Center, Japan Organization of Occupational Health and Safety, Kanagawa, Japan (J.K.); Analytical & Measuring Instruments Division, Shimadzu Corporation, Kyoto, Japan (T.Y.); Department of Biomedical Science, Institute of Regenerative Medicine and Biofunction, Graduate School of Medical Science, Tottori University, Tottori, Japan (Y.K.).

Molecular Pharmacology Fast Forward. Published on August 27, 2019 as DOI: 10.1124/mol.119.117333
This article has not been copyedited and formatted. The final version may differ from this version.

Running Title Page

Running title

Induction of CYP3A in double humanized mice of PXR and CYP3A

Corresponding author

Kaoru Kobayashi, Ph.D.

Laboratory of DDS Design and Drug Disposition, Graduate School of Pharmaceutical Sciences, Chiba University,

1-8-1 Inohana, Chuo-ku, Chiba 260-8675, Japan

Phone/Fax: +81-43-226-2895

E-mail: kaoruk@faculty.chiba-u.jp

Additional corresponding author

Yasuhiro Kazuki, Ph.D.

Department of Biomedical Science, Institute of Regenerative Medicine and Biofunction, Graduate School of Medical Science, Tottori University, 86 Nishi-cho, Yonago, Tottori 683-8503, Japan

Phone: +81-859-38-6219

Fax: +81-859-38-6210

E-mail: kazuki@tottori-u.ac.jp

The number of text pages: 31 pages

The number of tables: 2 tables

The number of figures: 4 figures

The number of references: 29 references

The number of words in Abstract: 218 words

The number of words in Introduction: 512 words

The number of words in Discussion: 1085 words

A list of nonstandard abbreviations

AUC: area under the plasma concentration-time curve, CAR: constitutive androstane receptor, CYP: cytochrome P450, DDI: drug-drug interaction, GAPDH: glyceraldehyde 3-phosphate dehydrogenase, KO: knockout, LC-MS/MS: liquid chromatography-tandem mass spectrometry, MAC: mouse artificial chromosome, PXR: pregnane X receptor, RIF: rifampicin, TRZ: triazolam.

Molecular Pharmacology Fast Forward. Published on August 27, 2019 as DOI: 10.1124/mol.119.117333
This article has not been copyedited and formatted. The final version may differ from this version.

Abstract

Induction of cytochrome P450 3A (CYP3A) in response to pregnane X receptor (PXR) activators shows species-specific differences. To study the induction of human CYP3A in response to human PXR activators, we generated a double humanized mouse model of PXR and CYP3A. CYP3A-humanized mice generated by using a mouse artificial chromosome (MAC) vector containing the entire genomic human CYP3A locus (hCYP3A-MAC mouse line) were bred with PXR-humanized mice in which the ligand binding domain of mouse PXR was replaced with that of human PXR, resulting in double humanized mice (hCYP3A-MAC/hPXR mouse line). Oral administration of the human PXR activator rifampicin increased hepatic expression of CYP3A4 mRNA and triazolam 1'- and 4-hydroxylation activities, CYP3A probe activities, in the liver and intestine microsomes of hCYP3A-MAC/hPXR mice. The plasma concentration of triazolam after oral dosing was significantly decreased by rifampicin treatment in hCYP3A-MAC/hPXR mice but not in hCYP3A-MAC mice. In addition, mass spectrometry imaging analysis showed that rifampicin treatment increased the formation of hydroxytriazolam in the intestine of hCYP3A-MAC/hPXR mice after oral dosing of triazolam. The plasma concentration of 1'- and 4-hydroxytriazolam in portal blood was also increased by rifampicin treatment in hCYP3A-MAC/hPXR mice. These

Molecular Pharmacology Fast Forward. Published on August 27, 2019 as DOI: 10.1124/mol.119.117333
This article has not been copyedited and formatted. The final version may differ from this version.

results suggest that the hCYP3A-MAC/hPXR mouse line may be a useful model to predict human PXR-dependent induction of metabolism of CYP3A4 substrates in the liver and intestine.

Molecular Pharmacology Fast Forward. Published on August 27, 2019 as DOI: 10.1124/mol.119.117333
This article has not been copyedited and formatted. The final version may differ from this version.

Significant Statement

We generated a double humanized mouse line for CYP3A and PXR. Briefly, CYP3A-humanized mice generated by using a mouse artificial chromosome vector containing the entire genomic human CYP3A locus were bred with PXR-humanized mice in which the ligand binding domain of mouse PXR was replaced with that of human PXR. Expression of CYP3A4 and metabolism of triazolam, a typical CYP3A substrate, in the liver of CYP3A/PXR-humanized mice were enhanced in response to rifampicin, a typical human PXR activator. Enhancement of triazolam metabolism in the intestine of CYP3A/PXR-humanized mice was firstly shown by combination of mass spectrometry imaging of sliced intestine and LC-MS/MS analysis of metabolite concentration in portal blood after oral dosing of triazolam.

Molecular Pharmacology Fast Forward. Published on August 27, 2019 as DOI: 10.1124/mol.119.117333
This article has not been copyedited and formatted. The final version may differ from this version.

Introduction

CYP3A4 is mainly expressed in the liver and intestine and contributes significantly to the pre-systemic elimination of drugs after oral administration (Thummel et al., 1996; von Richter et al., 2001). Since CYP3A4 is involved in the metabolism of about 50% of therapeutic drugs, inhibition or induction of CYP3A4 by concomitant drugs results in clinically important drug-drug interactions (DDIs) (Pelkonen *et al.*, 1998). Thus, regulatory agencies including the Food and Drug Administration, the European Medicines Agency, and the Pharmaceuticals and Medical Devices Agency of Japan have made recommendations in their DDI guidance documents for various methodologies to assess DDI potential (European Medicines Agency, 2012; Food and Drug Administration, 2017; Ministry of Health, Labour and Welfare, Japan, 2019).

Pregnane X receptor (PXR, NR1I2), a member of the nuclear receptor superfamily, regulates the induction process of CYP3A4 (Willson and Kliewer, 2002). PXR is activated by a broad range of chemicals such as steroid hormones, herbals and antibiotics (Mackowiak and Wang, 2016). Activated PXR translocates into the nucleus and forms a heterodimer with the retinoid X receptor alpha (RXRα). The PXR-RXRα heterodimer binds to DNA response elements and activates the transcription of target genes including *CYP3A4* (Goodwin *et al.*,

Molecular Pharmacology Fast Forward. Published on August 27, 2019 as DOI: 10.1124/mol.119.117333
This article has not been copyedited and formatted. The final version may differ from this version.

1999; Toriyabe et al., 2009). Interestingly, there are significant species differences in response to PXR activators between humans and rodents (Blumberg *et al.*, 1998; Kliewer *et al.*, 1998; Lehmann *et al.*, 1998; Jones *et al.*, 2000; Moore *et al.*, 2000; Quattrochi and Guzelian, 2001). The antibiotic rifampicin (RIF) activates human PXR but is a weak activator of rodent PXR. In contrast, pregnenolone16α-carbonitrile (PCN) potently activates rodent PXR but is a weak activator of human PXR. Since such differences lead to a problem for studies using rodents to predict DDIs in humans, some humanized mouse lines in which there are responses to human PXR activators have been developed (Cheung et al., 2006; Xie et al., 2000; Ma et al., 2008; Igarashi et al., 2012). Hasegawa et al. (2011) generated a multiple humanized mouse line that combines humanization of PXR and constitutive androstane receptor (CAR) and replacement of the mouse *Cyp3a* cluster with a human genomic region carrying *CYP3A4* and *CYP3A7* (huPXR/huCAR/huCYP3A4/3A7). The huPXR/huCAR/huCYP3A4/3A7 mice showed a CYP3A4 induction response to human PXR activators. In the huPXR/huCAR/huCYP3A4/3A7 mice, plasma concentrations of triazolam (TRZ), a typical CYP3A4 substrate, were decreased by oral administration of RIF. However, the induction of intestinal CYP3A4 mRNA expression was negligible when RIF was orally administered. In addition, the area under the plasma concentration-time curves (AUCs) of

Molecular Pharmacology Fast Forward. Published on August 27, 2019 as DOI: 10.1124/mol.119.117333
This article has not been copyedited and formatted. The final version may differ from this version.

TRZ metabolites were decreased by RIF treatment. Therefore, there is no direct evidence for enhancement of CYP3A4-mediated metabolism in the intestine of huPXR/huCAR/huCYP3A4/3A7 mice treated orally with human PXR activators.

In this study, we generated a double humanized mouse line for CYP3A and PXR and examined CYP3A4 induction in the liver and intestine of the double humanized mice in response to RIF. To demonstrate the functional induction of intestinal CYP3A4 by RIF, we determined the metabolite concentrations in portal blood after oral administration of TRZ and visualized the metabolite formation in the sliced small intestine by mass spectrometry imaging.

Molecular Pharmacology Fast Forward. Published on August 27, 2019 as DOI: 10.1124/mol.119.117333
This article has not been copyedited and formatted. The final version may differ from this version.

Materials and Methods

Materials

TRZ and RIF were purchased from Wako Pure Chemicals (Osaka, Japan). Pregnenolone 16α-carbonitrile (PCN) was purchased from Toronto Research Chemicals (North York, ON, Canada). 1'-Hydroxy TRZ and 4-hydroxy TRZ were supplied by Nihon Upjohn (Tokyo, Japan). All other reagents were purchased from commercial sources.

Animals

The generation and characterization of CYP3A-humanized mice and PXR-humanized mice were described previously (Kazuki et al., 2019; Igarashi et al. 2012). Briefly, a trans-chromosomic mouse line with a mouse artificial chromosome (MAC) vector containing the entire human *CYP3A* gene cluster (*CYP3A4, CYP3A5, CYP3A7* and *CYP3A43*) and their regulatory regions (promoters and enhancers) was crossed with Cyp3a-knockout (Cyp3a-KO) mice to produce CYP3A-humanized mice with a Cyp3a-knockout background (hCYP3A-MAC mouse line). The double humanized mice of CYP3A and PXR (hCYP3A-MAC/hPXR mouse line) and PXR-humanized mice with a Cyp3a-knockout background (Cyp3a-KO/hPXR mouse line) were generated by mating the

Molecular Pharmacology Fast Forward. Published on August 27, 2019 as DOI: 10.1124/mol.119.117333
This article has not been copyedited and formatted. The final version may differ from this version.

hCYP3A-MAC mouse line with a PXR-humanized mouse line in which the ligand-binding domain of mouse PXR was replaced with that of human PXR. Each mouse line was backcrossed to the C57BL/6 or ICR strain at least 6 generations. The primer sequences for the genomic PCR analyses are described in Supplemental Table 1. Primer sets for the genotyping of hCYP3A-MAC, Cyp3a-KO (double KO of Cyp3a57-59 and Cyp3a13) and hPXR-knock in, are described in Supplemental Table 2. All experiments were done using male mice between 10 and 11 weeks of age. Animals were kept in a temperature-controlled environment with a 12-hr light/dark cycle. The light-cycle hours were between 7 AM and 7 PM. They received a standard diet (CE-2, CLEA, Tokyo, Japan). The present study was conducted in accordance with the guidelines for the Care and Use of Laboratory Animals, as adopted by the Committee on Animal Research of Taiho Pharmaceutical Co., Tottori University and Chiba University.

Analysis of PXR-specific induction in the liver

hCYP3A-MAC mice and hCYP3A-MAC/hPXR mice were intraperitoneally treated with RIF (10 mg/kg, an hPXR activator), PCN (100 mg/kg, an mPXR activator) or a vehicle (corn oil) for four consecutive days. Sixteen hours after the final treatment, liver pieces were

Molecular Pharmacology Fast Forward. Published on August 27, 2019 as DOI: 10.1124/mol.119.117333
This article has not been copyedited and formatted. The final version may differ from this version.

collected.

Analysis of CYP3A4 induction by RIF in the liver and intestine

hCYP3A-MAC mice were orally treated with RIF (30 mg/kg) or a vehicle (0.5% carboxymethyl cellulose) for four consecutive days. Sixteen hours after the final treatment, the liver and small intestine were collected.

mRNA analysis

Total RNA was isolated from tissue pieces of livers and small intestines (1-cm segments collected at 10 cm from the pyloric region) by using the RNeasy Mini Kit (Qiagen, Germany). Reverse transcription was performed using a High-Capacity cDNA Reverse Transcription Kit (Thermo Fisher Scientific, Waltham, MA). CYP3A4 mRNA levels were determined by quantitative real-time PCR carried out on a CFX Connect Real-time System (Bio-Rad, Hercules, CA). The expression levels of CYP3A4 mRNA were determined by TaqMan probe-based real-time PCR using TaqMan Gene Expression Assays (Thermo Fisher Scientific, Hs00604506_m1). The mRNA expression levels were normalized to endogenous glyceraldehyde 3-phosphate dehydrogenase (GAPDH) gene expression detected by

Molecular Pharmacology Fast Forward. Published on August 27, 2019 as DOI: 10.1124/mol.119.117333
This article has not been copyedited and formatted. The final version may differ from this version.

20×Pre-Developed TaqMan Assay Reagent mouse GAPDH (Thermo Fisher Scientific).

TRZ hydroxylation activity *in vitro*

Microsomal fractions of the liver and intestine were prepared as described previously (Kazuki et al., 2013). Incubations were carried out in a total volume of 250 µl containing 0.1 mM EDTA, 100 mM potassium phosphate buffer (pH 7.4), an NADPH-generating system (0.5 mM $NADP^+$, 2 mM glucose-6-phosphate, 1 IU/ml glucose-6-phosphate dehydrogenase, 4 mM $MgCl_2$) and a substrate (200 µM TRZ). The microsomal protein concentrations and incubation times used were selected from the linear range of formation of TRZ metabolites. The mixtures were pre-incubated for 1 min at 37°C, and reactions were initiated by the addition of 25 µl of the NADPH-generation system. Incubation was stopped by the addition of 100 µl of acetonitrile followed by the addition of 50 µl of 1 µg/ml oxazepam in methanol as an internal control. Determination of 1'-hydroxy TRZ and 4-hydroxy TRZ was carried out using a Hitachi L-7000 model HPLC system (Tokyo, Japan) consisting an L-7400 UV detector and a CAPCELL PAK C18 UG120 column (4.6 mm x 250 mm, 5 mm; Shiseido, Tokyo, Japan). The mobile phase consisted of 10 mM potassium phosphate buffer (pH 7.4), acetonitrile and methanol (60/30/10, v/v/v), with a flow rate of 1.0

Molecular Pharmacology Fast Forward. Published on August 27, 2019 as DOI: 10.1124/mol.119.117333
This article has not been copyedited and formatted. The final version may differ from this version.

ml/min. The eluent was monitored at a wavelength of 220 nm.

Immunoblot analysis

Microsomal fractions (1 μg) of small intestines were separated by 10% SDS-polyacrylamide gel electrophoresis, transferred to a PVDF membrane, and probed using a mouse monoclonal anti-CYP3A4 antibody (1:1000 dilution, sc-53850, Santa Cruz Biotechnology, Dallas, TX) and a rabbit monoclonal anti-GAPDH antibody (1:10000 dilution, ab181602, Abcam, Cambridge, UK). The secondary antibodies used were horseradish peroxydase-conjugated rabbit anti-mouse IgG (1:5000 dilution, ab6728, Abcam) and goat anti-rabbit IgG (1:2000 dilution, ab6721, Abcam) for anti-CYP3A4 and anti-GAPDH, respectively. The primary and secondary antibodies were diluted with Can Get Signal Solution (TOYOBO, Osaka, Japan). CYP3A4 and GAPDH proteins were detected by an enhanced chemiluminescence method (GE Healthcare, Buckinghamshire, England) and LAS-4000 (Fujifilm, Tokyo, Japan). Intensities of bands were determined using ImageQuant TL (GE Healthcare).

Pharmacokinetic analysis

Molecular Pharmacology Fast Forward. Published on August 27, 2019 as DOI: 10.1124/mol.119.117333
This article has not been copyedited and formatted. The final version may differ from this version.

CYP3A-MAC/hPXR and hCYP3A-MAC mice were orally treated with TRZ (1 mg/kg) after oral administration of RIF (30 mg/kg/day) or a vehicle (0.5% carboxymethyl cellulose) for 3 consecutive days. Blood samples were collected from suborbital veins at 15, 30, 60, 120, 240 and 360 min after TRZ administration. Plasma was separated by centrifugation and stored at –80°C. The concentrations of TRZ, 1'-hydroxy TRZ and 4-hydroxy TRZ were determined by liquid chromatography-tandem mass spectrometry (LC-MS/MS) as described previously (Kazuki et al., 2019).

Area under the plasma concentration-time curve (AUC) from time 0 to the last data point (AUC0-t) was calculated using the linear trapezoidal method. $AUC_{0-\infty}$ was calculated by combining AUC_{0-t} and AUC_{extra}. AUC_{extra} represents an extrapolated value obtained by C_t/k_{el}, where C_t is the plasma concentration at the last data point and k_{el} represents the terminal elimination rate constant determined by log-linear regression analysis of the measured plasma concentrations of the terminal elimination phase. Maximum plasma concentration (Cmax) and time to Cmax (tmax) were obtained directly from the observed values. Apparent half-life was obtained as $\ln 2/k_{el}$.

Mass spectrometry imaging

Molecular Pharmacology Fast Forward. Published on August 27, 2019 as DOI: 10.1124/mol.119.117333
This article has not been copyedited and formatted. The final version may differ from this version.

The hCYP3A-MAC/hPXR mice were orally treated with RIF (10 mg/kg) or a vehicle (0.5% carboxymethyl cellulose) for 3 consecutive days. On Day 4, the mice were orally administered TRZ (10 mg/kg). At 10 min after TRZ administration, the liver and small intestine were quickly removed and frozen in liquid nitrogen. Serial sections were sliced to a thickness of 20 μm using a cryostat (CM 1950; Leica Microsystems, Wetzlar, Germany). Sections were thaw-mounted onto an indium-tin-oxide-coated glass slide (Sigma-Aldrich) and dried at room temperature. Before the mass spectrometry imaging, the samples were kept at –80°C. α-Cyano-4-hydroxycinnamic acid was used as the matrix-assisted laser desorption ionization matrix and was deposited by iMLayer (Shimadzu Corp., Kyoto, Japan). Mass imaging data were obtained using iMScope TRIO (Shimadzu). The mass range was set to m/z 300–400 with a spatial resolution of 20 μm.

Analysis of CYP3A-dependent induction in the intestine

CYP3A-MAC/hPXR and Cyp3a-KO/hPXR mice were orally treated with TRZ (1 mg/kg) after oral administration of RIF (30 mg/kg/day) or a vehicle (0.5% carboxymethyl cellulose) for 3 consecutive days. Blood samples were collected from portal veins at 10 min after TRZ administration. Plasma was separated by centrifugation and stored

Molecular Pharmacology Fast Forward. Published on August 27, 2019 as DOI: 10.1124/mol.119.117333
This article has not been copyedited and formatted. The final version may differ from this version.

at –80°C. The concentrations of TRZ, 1'-hydroxy TRZ and 4-hydroxy TRZ were determined by LC-MS/MS as described previously (Minegishi et al., 2019).

Statistical analysis

Data are expressed as means with S.D. Data were analyzed by using Statcel 4 (OMS, Saitama, Japan) and R 3.5.1 (R Foundation for Statistical Computing, Vienna, Austria). Comparisons of two groups were performed using a two-tailed *t*-test. Comparisons of multiple groups were performed by MANOVA followed by one-way ANOVA with a post-hoc test. $P < 0.05$ was considered statistically significant.

Results

Human PXR-dependent induction of hepatic CYP3A in hCYP3A-MAC/hPXR mice

hCYP3A-MAC/hPXR and hCYP3A-MAC mice were intraperitoneally treated with the human PXR ligand RIF and rodent PXR ligand PCN. After PCN treatment, CYP3A4 mRNA was significantly increased in the liver of hCYP3A-MAC mice but not in hCYP3A-MAC/hPXR mice (Fig. 1A). In contrast, RIF treatment did not increase CYP3A4 mRNA in hCYP3A-MAC mice, whereas an increase of CYP3A4 mRNA was found in

Molecular Pharmacology Fast Forward. Published on August 27, 2019 as DOI: 10.1124/mol.119.117333
This article has not been copyedited and formatted. The final version may differ from this version.

hCYP3A-MAC/hPXR mice, though the increase was not statistically significant. Consistent with CYP3A4 expression, TRZ 1'- and 4-hydroxylation activities, marker activities of CYP3A, increased significantly in the liver microsomes of hCYP3A-MAC mice after PCN treatment but not after RIF treatment (Fig. 1B). In hCYP3A-MAC/hPXR mice, TRZ 1'- and 4-hydroxylation activities increased after RIF treatment but not after PCN treatment. These results showed that the response of human CYP3A4 expression to PXR activators in the liver of hCYP3A-MAC/hPXR mice mimicked the response in hPXR.

Effect of RIF on CYP3A4 expression in the liver and intestine of hCYP3A-MAC/hPXR mice

Next, we examined the induction of CYP3A4 in the liver and intestine of hCYP3A-MAC/hPXR mice after oral treatment with RIF. A significant increase of CYP3A4 mRNA levels induced by RIF was observed in the liver of hCYP3A-MAC/hPXR mice (Fig. 2A). Hepatic CYP3A activity was also significantly induced by RIF in hCYP3A-MAC/hPXR mice (Fig. 2B). In the intestine, a significant increase of CYP3A activity was observed, but the magnitude of increase was less than that in the liver. No increase of CYP3A4 mRNA with RIF

treatment was found in the intestine (Fig. 2A), although CYP3A4 protein was marginally increased by RIF in the intestine of CYP3A-MAC/hPXR mice (Supplemental Figure 1).

Effect of RIF on pharmacokinetics of TRZ in hCYP3A-MAC/hPXR mice

To assess whether RIF can affect the pharmacokinetics of TRZ and its metabolites in hCYP3A-MAC/hPXR mice, hCYP3A-MAC mice and hCYP3A-MAC/hPXR mice were orally administered TRZ after oral daily doses of the vehicle or RIF for three days. Since the plasma concentration of 4-hydroxy TRZ in hCYP3A-MAC mice was lower than the quantification limit (250 nM), the plasma concentration-time curves for TRZ and 1'-hydroxy TRZ are shown in Fig. 3, and the pharmacokinetic parameters are summarized in Tables 1 and 2. The $AUC_{0-\infty}$ value of TRZ was significantly decreased by RIF treatment in hCYP3A-MAC/hPXR mice (76% decrease). The half-life of TRZ was also decreased by RIF. On the other hand, no significant effects of RIF on the $AUC_{0-\infty}$ value and half-life of TRZ were observed in hCYP3A-MAC mice. These results showed that the decreases of the $AUC_{0-\infty}$ value and half-life of TRZ were human PXR-dependent.

Induction of intestinal CYP3A by RIF in hCYP3A-MAC/hPXR mice

Molecular Pharmacology Fast Forward. Published on August 27, 2019 as DOI: 10.1124/mol.119.117333
This article has not been copyedited and formatted. The final version may differ from this version.

To investigate the enhancement of TRZ metabolism in the intestine of hCYP3A-MAC/hPXR mice, we tried to visualize the metabolism of TRZ in the intestine by mass spectrometry imaging. As shown Fig. 4A, the signal intensity of hydroxy TRZ increased in the sliced intestine of hCYP3A-MAC/hPXR mice treated with RIF.

Furthermore, we investigated whether the enhancement of TRZ metabolism in the intestine of hCYP3A-MAC/hPXR mice treated with RIF is CYP3A-dependent. The hCYP3A-MAC/hPXR mice and Cyp3a-KO/hPXR mice were orally administered the vehicle or RIF for three days. At 10 min after oral administration of TRZ, the plasma concentrations of TRZ and its metabolites in portal blood were determined. As shown in Fig. 4B, the plasma concentration of TRZ in portal blood was decreased in hCYP3A-MAC/hPXR mice. The plasma concentrations of 1'-hydroxy TRZ and 4-hydroxy TRZ in portal blood, which showed first-pass metabolism in the small intestine, were increased by RIF treatment in hCYP3A-MAC/hPXR mice (Fig. 4C). We still found a significant decrease of TRZ concentration in the portal blood of Cyp3a-KO/hPXR mice treated with RIF (Supplemental Figure 2A). The plasma concentrations of 1'-hydroxy TRZ and 4-hydroxy TRZ in portal blood were also increased by RIF treatment in Cyp3a-KO/hPXR mice, although the concentrations were lower than those in hCYP3A-MAC/hPXR mice (Supplemental Figure 2B).

Molecular Pharmacology Fast Forward. Published on August 27, 2019 as DOI: 10.1124/mol.119.117333
This article has not been copyedited and formatted. The final version may differ from this version.

Discussion

We previously reported an hCYP3A-MAC mouse model with a mouse PXR background (Kazuki et al., 2019, Minegishi et al., 2019). In contrast to the hCYP3A-MAC mouse model, the present hCYP3A-MAC/hPXR mouse model was improved as a mouse line with a human PXR-like response. Therefore, the hCYP3A-MAC/hPXR mouse model would be a useful tool for the study of CYP3A4 induction by human PXR activators.

The present study clearly showed that plasma concentrations of TRZ were decreased by RIF only in the hCYP3A-MAC/hPXR mice (Fig. 3A and 3B), suggesting that oral clearance of TRZ was enhanced in response to hPXR activation by RIF. In hCYP3A-MAC/hPXR mice, hepatic CYP3A4 mRNA levels and TRZ metabolism in the liver microsomes were increased by oral treatment with RIF (Fig. 2), being consistent with previous results obtained from humanized mouse models for PXR accomplished using different strategies (Ma et al., 2008; Hasegawa et al., 2011). Plasma elimination of TRZ after oral dosing was also enhanced by RIF in hCYP3A-MAC/hPXR mice (Table 1). These findings suggested induction of CYP3A4-mediated metabolism of TRZ in the liver of hCYP3A-MAC/hPXR mice. In addition, TRZ metabolism and CYP3A4 protein in the intestinal microsomes were also increased by oral treatment with RIF (Fig. 2B and Supplemental Figure

Molecular Pharmacology Fast Forward. Published on August 27, 2019 as DOI: 10.1124/mol.119.117333
This article has not been copyedited and formatted. The final version may differ from this version.

1). Results of mass spectrometry imaging analysis demonstrated that hydroxy TRZ in the sliced intestine of hCYP3A-MAC/hPXR mice was increased by treatment with RIF (Fig. 4A). Moreover, the plasma concentrations of TRZ and its metabolites in portal blood were decreased and increased, respectively, by RIF in hCYP3A-MAC/hPXR mice (Fig. 4B and 4C). Although metabolites found in blood of the portal vein were not always derived from the mesenteric vein, the concentrations of metabolites at 10 min after oral administration would reflect the intestinal metabolism. Since these experiments were performed for hCYP3A-MAC/hPXR mice, we cannot exclude the possibility that the induction of intestinal metabolism is hPXR-independent. However, plasma concentrations of 1'-hydroxy TRZ at the early phase after TRZ dosing were increased by RIF treatment in hCYP3A-MAC/hPXR mice but not in hCYP3A-MAC mice (Figs. 3C and D). In addition, RIF could not induce CYP3A in Pxr-null mice (Ma et al., 2007). These findings suggested that TRZ metabolism in the intestine of hCYP3A-MAC/hPXR mice was enhanced in response to hPXR activation by RIF. Therefore, the present study firstly showed that the overall metabolism of TRZ in the liver and intestine was functionally enhanced by oral administration of RIF in hCYP3A-MAC/hPXR mice.

In agreement with previously reported findings in huPXR/huCAR/huCYP3A4/3A7

Molecular Pharmacology Fast Forward. Published on August 27, 2019 as DOI: 10.1124/mol.119.117333
This article has not been copyedited and formatted. The final version may differ from this version.

mice (Hasegawa et al., 2011), the $AUC_{0-\infty}$ value and half-life of 1'-hydroxy TRZ were also decreased by RIF treatment in hCYP3A-MAC/hPXR mice (Table 2). Notably, our results indicated a trend for plasma concentrations of 1'-hydroxy TRZ at 15 and 30 min after TRZ dosing to be increased by RIF treatment in hCYP3A-MAC/hPXR mice (Fig. 3C). These results take together with results showing enhanced formation of 1'-hydroxy TRZ in the intestine of hCYP3A-MAC/hPXR mice treated with RIF (Fig. 4) suggested that formation of 1'-hydroxy TRZ in intestinal metabolism was enhanced and subsequently further metabolism of 1'-hydroxy TRZ was enhanced in the liver of hCYP3A-MAC/hPXR mice treated with RIF.

Previously, Hasegawa et al. (2011) reported that huPXR/huCAR/huCYP3A4/3A7 mice showed a CYP3A4 induction response to human PXR activators, but the induction of intestinal CYP3A4 mRNA expression was not significant when RIF was orally administered. Ma et al. (2007 and 2008) also reported a PXR-humanized mouse model and a double transgenic mouse model expressing human PXR and CYP3A4, but they showed no data for the induction of CYP3A4 mRNA in the intestine. Consistent with these findings, the present study using hCYP3A-MAC/hPXR mice also showed that the induction of intestinal CYP3A4 mRNA expression was not significant when RIF was orally administered (Fig. 2A). On the other hand, expression of intestinal CYP3A protein was increased in hCYP3A-MAC/hPXR

Molecular Pharmacology Fast Forward. Published on August 27, 2019 as DOI: 10.1124/mol.119.117333
This article has not been copyedited and formatted. The final version may differ from this version.

mice (supplemental Figure 1) as well as previous mouse models (Ma et al., 2007 and 2008; Hasegawa et al., 2011) when RIF was orally administered. Therefore, it may be difficult to detect the induction of CYP3A4 at the mRNA level in the intestine of mouse models treated with RIF.

Metabolic activities of TRZ in intestinal microsomes were increased by RIF in hCYP3A-MAC/hPXR mice (Fig. 2B), but we could not exclude the possibility that TRZ was metabolized by other genes that were induced by RIF in hCYP3A-MAC/hPXR mice. Therefore, we investigated the induction of intestinal CYP3A4 by RIF in hCYP3A-MAC/hPXR mice by comparing the plasma concentrations of TRZ and its metabolites in portal blood between hCYP3A-MAC/hPXR mice and Cyp3a-KO/hPXR mice. In the present study, the plasma concentration of 1'-hydroxy TRZ and 4-hydroxy TRZ in portal blood after 10 min of dosing was detected in both Cyp3a-KO/hPXR and hCYP3A-MAC/hPXR mice (Fig. 4C and Supplemental Figure 2B). We still observed increases of 1'-hydroxy TRZ and 4-hydroxy TRZ in portal blood in Cyp3a-KO/hPXR mice by RIF. These results suggest that RIF-inducible enzymes other than CYP3A contribute to TRZ metabolism in Cyp3a-KO/hPXR mice. It has been reported that expression levels of some genes including mouse Cyp2c enzymes could be increased by KO of *Cyp3a* genes and by treatment with PXR activators (Waterschoot et al.,

2009; Minegishi et al., 2019). In addition, an anti-CYP2C antibody inhibited TRZ hydroxylation activities in Cyp3a-KO mice but not in wild-type mice (Minegishi et al., 2019). These findings implied that the mouse Cyp2c enzymes were involved in TRZ metabolism in Cyp3a-KO/hPXR mice. To exclude the possibility of contribution of enzymes other than CYP3A to TRZ metabolism in mice with a Cyp3a-KO background, further modifications such as a combination with KO of other genes are needed.

The hCYP3A-MAC/hPXR mice used in this study have not only the *CYP3A4* gene but also *CYP3A5*, *CYP3A7* and *CYP3A43* genes. CYP3A5 shows polymorphic expression in the adult liver (Kuehl et al., 2001). Since hCYP3A-MAC/hPXR mice have a 6986A>G mutation in the *CYP3A5*3* allele, the expression level of CYP3A5 protein is negligible. Recently, we generated CYP3A-MAC mice with *CYP3A5*1* by genome editing technology (Abe et al., 2017). Since CYP3A5 could be induced by RIF (Burk et al., 2004), further studies for comparison of induction between CYP3A4 and CYP3A5 *in vivo* may be accomplished by generation of a mouse model containing *CYP3A5*1* and hPXR.

In conclusion, the present study demonstrated that oral treatment with RIF to hCYP3A-MAC/hPXR mice enhanced TRZ metabolism in the intestine as well as the liver in response to hPXR activation. The hCYP3A-MAC/hPXR mouse line will be a useful *in vivo*

Molecular Pharmacology Fast Forward. Published on August 27, 2019 as DOI: 10.1124/mol.119.117333
This article has not been copyedited and formatted. The final version may differ from this version.

model for predicting the induction of hepatic and intestinal metabolism of CYP3A substrates *via* human PXR activation.

Acknowledgments

We thank Kanako Takano at Chiba University and Toko Kurosaki, Yukako Sumida, Hiromichi Kohno, Masami Morimura, Kei Yoshida, Eri Kaneda, Akiko Ashiba, and Dr. Kazuomi Nakamura, at Tottori University for technical assistance in the experiment. We also thank Dr. Kan Chiba at Chiba University and Dr. Hiroyuki Kugoh, Dr. Masaharu Hiratsuka, Dr. Tetsuya Ohbayashi, and Dr. Takahito Ohira at Tottori University for critical discussion and Dr. Akihiro Hisaka and Shizuka Hozuki at Chiba University for critical support in the statistical analysis. This research was partly performed at the Tottori Bio Frontier managed by Tottori prefecture.

Molecular Pharmacology Fast Forward. Published on August 27, 2019 as DOI: 10.1124/mol.119.117333
This article has not been copyedited and formatted. The final version may differ from this version.

Authorship Contributions

Participated in research design: Kobayashi, Kuze, Kazuki.

Conducted experiments: Kuze, Takehara, Minegishi, Igarashi, Kitajima, Kanno, Yamamoto.

Performed data analysis: Kobayashi, Kuze, Abe, Yamamoto.

Wrote or contributed to the writing of the manuscript: Kobayashi, Abe, Yamamoto, Oshimura, Kazuki.

Molecular Pharmacology Fast Forward. Published on August 27, 2019 as DOI: 10.1124/mol.119.117333
This article has not been copyedited and formatted. The final version may differ from this version.

References

Abe S, Kobayashi K, Oji A, Sakuma T, Kazuki K, Takehara S, Nakamura K, Okada A, Tsukazaki Y, Senda N, Honma K, Yamamoto T, Ikawa M, Chiba K, Oshimura M, Kazuki Y (2017) Modification of single-nucleotide polymorphism in a fully humanized CYP3A mouse by genome editing technology. *Sci Rep* **7:** 15189.

Blumberg B, Sabbagh W Jr, Juguilon H, Bolado J Jr, van Meter CM, Ong ES, and Evans RM (1998) SXR, a novel steroid and xenobiotic-sensing nuclear receptor. *Genes Dev* **12:**3195-3205.

Burk O, Koch I, Raucy J, Hustert E, Eichelbaum M, Brockmöller J, Zanger UM, and Wojnowski L (2004) The induction of cytochrome P450 3A5 (CYP3A5) in the human liver and intestine is mediated by the xenobiotic sensors pregnane X receptor (PXR) and constitutively activated receptor (CAR). *J Biol Chem* **279:** 38379-38385.

Cheung C, Yu AM, Chen CS, Krausz KW, Byrd LG, Feigenbaum L, Edwards RJ, Waxman DJ, Gonzalez FJ (2006) Growth hormone determines sexual dimorphism of hepatic

cytochrome P450 3A4 expression in transgenic mice. *J Pharmacol Exp Ther* **316:**1328-1334.

European Medicines Agency (2012) Guideline on the investigation of drug interactions. (Available at: http://www.ema.europa.eu/docs/en_GB/document_library/Scientific_guideline/2012/07/WC500129606.pdf)

Food and Drug Administration (2017) Draft guidance/guidance for industry. Drug interaction studies–study design, data analysis, implications for dosing, and labeling recommendations. (Available at: http://www.fda.gov/downloads/Drugs/GuidanceComplianceRegulatoryInformation/Guidances/UCM292362.pdf)

Goodwin B, Hodgson E, and Liddle C (1999) The orphan human pregnane X receptor mediates the transcriptional activation of CYP3A4 by rifampicin through a distal enhancer module. *Mol Pharmacol* **56:** 1329-1339.

Molecular Pharmacology Fast Forward. Published on August 27, 2019 as DOI: 10.1124/mol.119.117333
This article has not been copyedited and formatted. The final version may differ from this version.

Hasegawa M, Kapelyukh Y, Tahara H, Seibler J, Rode A, Krueger S, Lee DN, Wolf CR, and Scheer N (2011) Quantitative prediction of human pregnane X receptor and cytochrome P450 3A4 mediated drug-drug interaction in a novel multiple humanized mouse line. *Mol Pharmacol* **80:** 518-528.

Igarashi K, Kitajima S, Aisaki K, Tanemura K, Taquahashi Y, Moriyama N, Ikeno E, Matsuda N, Saga Y, Blumberg B, and Kanno J (2012) Development of humanized steroid and xenobiotic receptor mouse by homologous knock-in of the human steroid and xenobiotic receptor ligand binding domain sequence. *J Toxicol Sci* **37:**373-380.

Jones SA, Moore LB, Shenk JL, Wisely GB, Hamilton GA, McKee DD, Tomkinson NC, LeCluyse EL, Lambert MH, Willson TM, Kliewer SA, and Moore JT (2000) The pregnane X receptor: a promiscuous xenobiotic receptor that has diverged during evolution. *Mol Endocrinol* **14:** 27-39.

Kazuki Y, Kobayashi K, Aueviriyavit S, Oshima T, Kuroiwa Y, Tsukazaki Y, Senda N, Kawakami H, Ohtsuki S, Abe S, Takiguchi M, Hoshiya H, Kajitani N, Takehara S, Kubo K, Terasaki T, Chiba K, Tomizuka K, and Oshimura M (2013) Trans-chromosomic mice containing a human CYP3A cluster for prediction of xenobiotic metabolism in humans. *Hum Mol Genet* **22:** 578-592.

Kazuki Y, Kobayashi K, Hirabayashi M, Abe S, Kajitani N, Kazuki K, Takehara S, Takiguchi M, Satoh D, Kuze J, Sakuma T, Kaneko T, Mashimo T, Osamura M, Hashimoto M, Wakatsuki R, Hirashima R, Fujiwara R, Deguchi T, Kurihara A, Tsukazaki Y, Senda N, Yamamoto T, Scheer N, and Oshimura M (2019) Humanized UGT2 and CYP3A transchromosomic rats for improved prediction of human drug metabolism. *Proc Natl Acad Sci USA* **116:** 3072-3081.

Kliewer SA, Moore JT, Wade L, Staudinger JL, Watson MA, Jones SA, McKee DD, Oliver BB, Willson TM, Zetterström RH, Perlmann T, and Lehmann JM (1998) An orphan nuclear receptor activated by pregnanes defines a novel steroid signaling pathway. *Cell* **92:** 73-82.

Kuehl P, Zhang J, Lin Y, Lamba J, Assem M, Schuetz J, Watkins PB, Daly A, Wrighton SA, Hall SD, Maurel P, Relling M, Brimer C, Yasuda K, Venkataramanan R, Strom S, Thummel K, Boguski MS, and Schuetz E (2001) Sequence diversity in CYP3A promoters and characterization of the genetic basis of polymorphic CYP3A5 expression. *Nat Genet* **27:** 383-391.

Lehmann JM, McKee DD, Watson MA, Willson TM, Moore JT, and Kliewer SA (1998) The human orphan nuclear receptor PXR is activated by compounds that regulate CYP3A4 gene expression and cause drug interactions. *J Clin Invest* **102:** 1016-1023.

Ma X, Cheung C, Krausz KW, Shah YM, Wang T, Idle JR, and Gonzalez FJ (2008) A double transgenic mouse model expressing human pregnane X receptor and cytochrome P450 3A4. *Drug Metab Dispos* **36:** 2506-2512.

Ma X, Shah Y, Cheung C, Guo GL, Feigenbaum L, Krausz KW, Idle JR, Gonzalez FJ (2007) The pregnane X receptor gene-humanized mouse: a model for investigating drug-drug interactions mediated by cytochromes P450 3A. Drug Metab Dispos 35:194-200.

Mackowiak B and Wang H (2016) Mechanisms of xenobiotic receptor activation: Direct vs. indirect. *Biochim Biophys Acta* **1859:** 1130-1140.

Minegishi G, Kazuki Y, Yamasaki Y, Okuya F, Akita H, Oshimura M, and Kobayashi K (2019) Comparison of the hepatic metabolism of TRZ in wild-type and Cyp3a-knockout mice for understanding CYP3A-mediated metabolism in CYP3A-humanized mice in vivo. *Xenobiotica* doi: 10.1080/00498254.2018.1560516.

Ministry of Health, Labour and Welfare, Japan (2019) Guideline on drug interaction for drug development and appropriate provision of information. (Available at: http://www.pmda.go.jp/files/000228122.pdf)

Moore LB, Parks DJ, Jones SA, Bledsoe RK, Consler TG, Stimmel JB, Goodwin B, Liddle C, Blanchard SG, Willson TM, Collins JL, and Kliewer SA (2000) Orphan nuclear receptors constitutive androstane receptor and pregnane X receptor share xenobiotic and steroid ligands. *J Biol Chem* **275:** 15122-15127.

Pelkonen O, Mäenpää J, Taavitsainen P, Rautio A, and Raunio H (1998) Inhibition and induction of human cytochrome P450 (CYP) enzymes. *Xenobiotica* **28:** 1203-1253.

Quattrochi LC and Guzelian PS (2001) Cyp3A regulation: from pharmacology to nuclear receptors. *Drug Metab Dispos* **29:** 615-622.

Thummel KE, O'Shea D, Paine MF, Shen DD, Kunze KL, Perkins JD, and Wilkinson GR (1996) Oral first-pass elimination of midazolam involves both gastrointestinal and hepatic CYP3A-mediated metabolism. *Clin Pharmacol Ther* **59:** 491-502.

Toriyabe T, Nagata K, Takada T, Aratsu Y, Matsubara T, Yoshinari K, and Yamazoe Y (2009) Unveiling a new essential cis element for the transactivation of the CYP3A4 gene by xenobiotics. *Mol Pharmacol* **75:** 677-684.

van Waterschoot RA, Rooswinkel RW, Wagenaar E, van der Kruijssen CM, van Herwaarden AE, and Schinkel AH (2009) Intestinal cytochrome P450 3A plays an important role in the regulation of detoxifying systems in the liver. *FASEB J* **23:** 224-231.

von Richter O, Greiner B, Fromm MF, Fraser R, Omari T, Barclay ML, Dent J, Somogyi AA, and Eichelbaum M (2001) Determination of in vivo absorption, metabolism, and transport of drugs by the human intestinal wall and liver with a novel perfusion technique. *Clin Pharmacol Ther* **70:** 217-227.

Willson TM and Kliewer SA (2002) PXR, CAR and drug metabolism. *Nat Rev Drug Discov* **1:** 259-266.

Molecular Pharmacology Fast Forward. Published on August 27, 2019 as DOI: 10.1124/mol.119.117333
This article has not been copyedited and formatted. The final version may differ from this version.

Xie W, Barwick JL, Downes M, Blumberg B, Simon CM, Nelson MC, Neuschwander-Tetri BA, Brunt EM, Guzelian PS, and Evans RM (2000) Humanized xenobiotic response in mice expressing nuclear receptor SXR. *Nature* **406:** 435-439.

.

Molecular Pharmacology Fast Forward. Published on August 27, 2019 as DOI: 10.1124/mol.119.117333
This article has not been copyedited and formatted. The final version may differ from this version.

Footnotes

This work was supported in part by the Regional Innovation Strategy Support Program from MEXT (Y.K. and M.O.), the Funding Program for Next Generation World-Leading Researchers (NEXT Program) from the JSPS (Y.K.), the Basis for Supporting Innovative Drug Discovery and Life Science Research (BINDS) from Japan Agency for Medical Research and Development (AMED) under Grant Number JP18am0301009 (YK) and AMED under Grant Number JP19fk0310112 (KK).

Molecular Pharmacology Fast Forward. Published on August 27, 2019 as DOI: 10.1124/mol.119.117333
This article has not been copyedited and formatted. The final version may differ from this version.

Figure legends

Fig. 1 CYP3A4 mRNA and CYP3A marker activities in the liver of hCYP3A-MAC and hCYP3A-MAC/hPXR mice.

Mice (*N* = 3/group except for *N* = 5/hCYP3A-MAC treated with oil and *N* = 4/hCYP3A-MAC treated with RIF) were treated by intraperitoneal injection of a vehicle (corn oil), PCN (100 mg/kg) or RIF (10 mg/kg) for 4 days. A. CYP3A4 mRNA expression level was normalized by GAPDH. B. Formation rates of 1'-hydroxy TRZ (1'-OH) and 4-hydroxy TRZ (4-OH) from TRZ (200 μM) were determined by using liver microsomes as CYP3A marker activities. Data are expressed as means with S.D. Statistical analysis was firstly performed with MANOVA. Then one-way ANOVA with Scheffe's F test was performed for mRNA, 1'-OH and 4-OH in hCYP3A-MAC and hCYP3A-MAC/hPXR mice, respectively. **, $p < 0.01$ compared with the mRNA value of hCYP3A-MAC mice (hCYP3A/mPXR) treated with a vehicle. ††, $p < 0.01$ compared with 1'-OH of hCYP3A-MAC mice treated with a vehicle. ‡‡, $p < 0.01$ compared with 4-OH of hCYP3A-MAC mice treated with a vehicle.

Fig. 2 CYP3A4 mRNA and metabolic activity of CYP3A4 probe substrate in the liver and intestine of hCYP3A-MAC/hPXR mice.

Molecular Pharmacology Fast Forward. Published on August 27, 2019 as DOI: 10.1124/mol.119.117333
This article has not been copyedited and formatted. The final version may differ from this version.

Mice (*N* = 3/group) were orally treated with either a vehicle (0.5% CMC) or RIF (30 mg/kg) for 3 days. A. The CYP3A4 mRNA expression level was normalized by GAPDH. B. Formation rates of 1'-hydroxy TRZ (1'-OH) and 4-hydroxy TRZ (4-OH) from TRZ (200 μM) were determined by using liver and intestine microsomes. Data are expressed as means with S.D. Statistical analysis was performed with two-tailed *t* test. *, $p < 0.05$ compared with the mRNA value in the liver of hCYP3A-MAC/hPXR mice treated with a vehicle (Welch's *t* test). † and ‡, $p < 0.05$ compared with 1'-OH and 4-OH, respectively, in the liver of hCYP3A-MAC/hPXR mice treated with a vehicle (Welch's *t* test). †† and ‡‡, $p < 0.01$ compared with 1'-OH and 4-OH, respectively, in the intestine of hCYP3A-MAC/hPXR mice treated with a vehicle (Student's *t* test).

Fig. 3 Plasma concentration-time profiles of TRZ (A and B) and 1'-hydroxy TRZ (C and D) in hCYP3A-MAC/hPXR (A and C) and hCYP3A-MAC (B and D) mice.

Mice (*N* = 3/group for hCYP3A-MAC/hPXR mice and *N* = 4/group for hCYP3A-MAC mice) were given an oral dose of the vehicle or RIF (30 mg/kg) for three days followed by 1 mg/kg oral dose of TRZ. Values for the vehicle are indicated as open circles and those for RIF are indicated as closed circles. Each point represents the means with S.D.

Molecular Pharmacology Fast Forward. Published on August 27, 2019 as DOI: 10.1124/mol.119.117333
This article has not been copyedited and formatted. The final version may differ from this version.

Fig. 4 Induction of TRZ metabolism in the small intestine of hCYP3A-MAC/hPXR mice.

A. Imaging mass spectrometry of TRZ and its hydroxy metabolites in the small intestine. hCYP3A-MAC/hPXR mice (*N* = 1/group) were given an oral dose of the vehicle or RIF (30 mg/kg) for three days followed by 10 mg/kg oral dose of TRZ. At 10 min after TRZ dosing, the small intestine was removed and analyzed as described in the Methods section. B and C. Plasma concentrations of TRZ (B) and its metabolites 1'-hydroxy TRZ and 4-hydroxy TRZ (C) in portal blood of hCYP3A-MAC/hPXR mice. Mice (*N* = 4/group) were given an oral dose of the vehicle or RIF (30 mg/kg) for three days followed by 1 mg/kg oral dose of TRZ. At 10 min after TRZ dosing, blood samples were collected from portal veins. Data are expressed as means with S.D. Statistical analysis was performed with Student's *t* test. *, $p < 0.05$ compared with the vehicle control. ††, $p < 0.01$ compared with 1'-OH of hCYP3A-MAC/hPXR mice treated with a vehicle. ‡‡, $p < 0.01$ compared with 4-OH of hCYP3A-MAC/hPXR mice treated with a vehicle.

Molecular Pharmacology Fast Forward. Published on August 27, 2019 as DOI: 10.1124/mol.119.117333
This article has not been copyedited and formatted. The final version may differ from this version.

Table 1 Pharmacokinetic parameters of TRZ in hCYP3A-MAC/hPXR and hCYP3A-MAC mice

Group	t_{max} (hr)	C_{max} (nM)	half-life (hr)	$AUC_{0-\infty}$ (nM•hr)
hCYP3A-MAC/hPXR				
vehicle	0.42 ± 0.14	515 ± 190	1.10 ± 0.14	1050 ± 242
RIF	0.50 ± 0.43	235 ± 55	0.39 ± 0.05**	250 ± 71**
hCYP3A-MAC				
vehicle	0.38 ± 0.14	229 ± 81	1.08 ± 0.13	448 ± 157
RIF	0.44 ± 0.13	180 ± 22	1.21 ± 0.44	370 ± 82

hCYP3A-MAC/hPXR and hCYP3A-MAC mice were administered the vehicle or RIF followed by 1 mg/kg oral dose of TRZ. Data represent means ± S.D. (*N* = 3/group for hCYP3A-MAC/hPXR mice and *N* = 4/group for hCYP3A-MAC mice). **, $p < 0.01$ compared with the vehicle control (Student's *t* test).

Molecular Pharmacology Fast Forward. Published on August 27, 2019 as DOI: 10.1124/mol.119.117333
This article has not been copyedited and formatted. The final version may differ from this version.

Table 2 Pharmacokinetic parameters of 1'-hydroxy TRZ in hCYP3A-MAC/hPXR and hCYP3A-MAC mice

Group	t_{max} (hr)	C_{max} (nM)	half-life (hr)	$AUC_{0-\infty}$ (nM•hr)
hCYP3A-MAC/hPXR				
vehicle	1.33 ± 0.58	978 ± 200	3.25 ± 0.50	4893 ± 1062
RIF	0.58 ± 0.38	1250 ± 414	0.64 ± 0.14***	1737 ± 27*
hCYP3A-MAC				
vehicle	0.63 ± 0.25	747 ± 165	2.19 ± 0.43	2618 ± 738
RIF	0.88 ± 0.25	712 ± 47	2.07 ± 0.38	2313 ± 562

hCYP3A-MAC/hPXR and hCYP3A-MAC mice were administered the vehicle or RIF followed by 1 mg/kg oral dose of TRZ. Data represent means ± S.D. (*N* = 3/group for hCYP3A-MAC/hPXR mice and *N* = 4/group for hCYP3A-MAC mice). *, $p < 0.05$ and ***, $p < 0.001$ compared with the vehicle control (Student's *t* test for half-life and Welch's *t* test for AUC).

Molecular Pharmacology Fast Forward. Published on August 27, 2019 as DOI: 10.1124/mol.119.117333
This article has not been copyedited and formatted. The final version may differ from this version.

Fig. 1

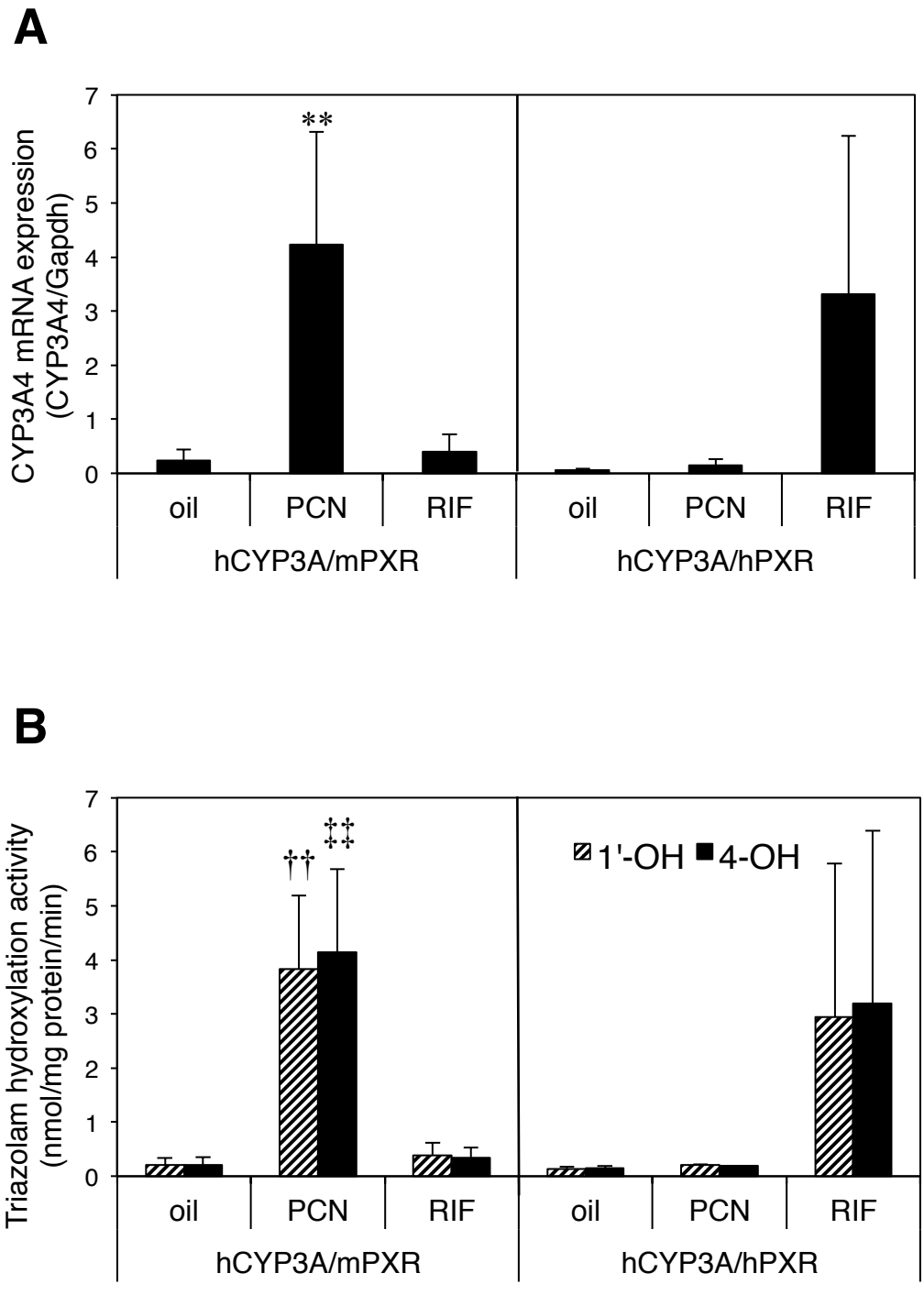

Molecular Pharmacology Fast Forward. Published on August 27, 2019 as DOI: 10.1124/mol.119.117333
This article has not been copyedited and formatted. The final version may differ from this version.

Fig. 2

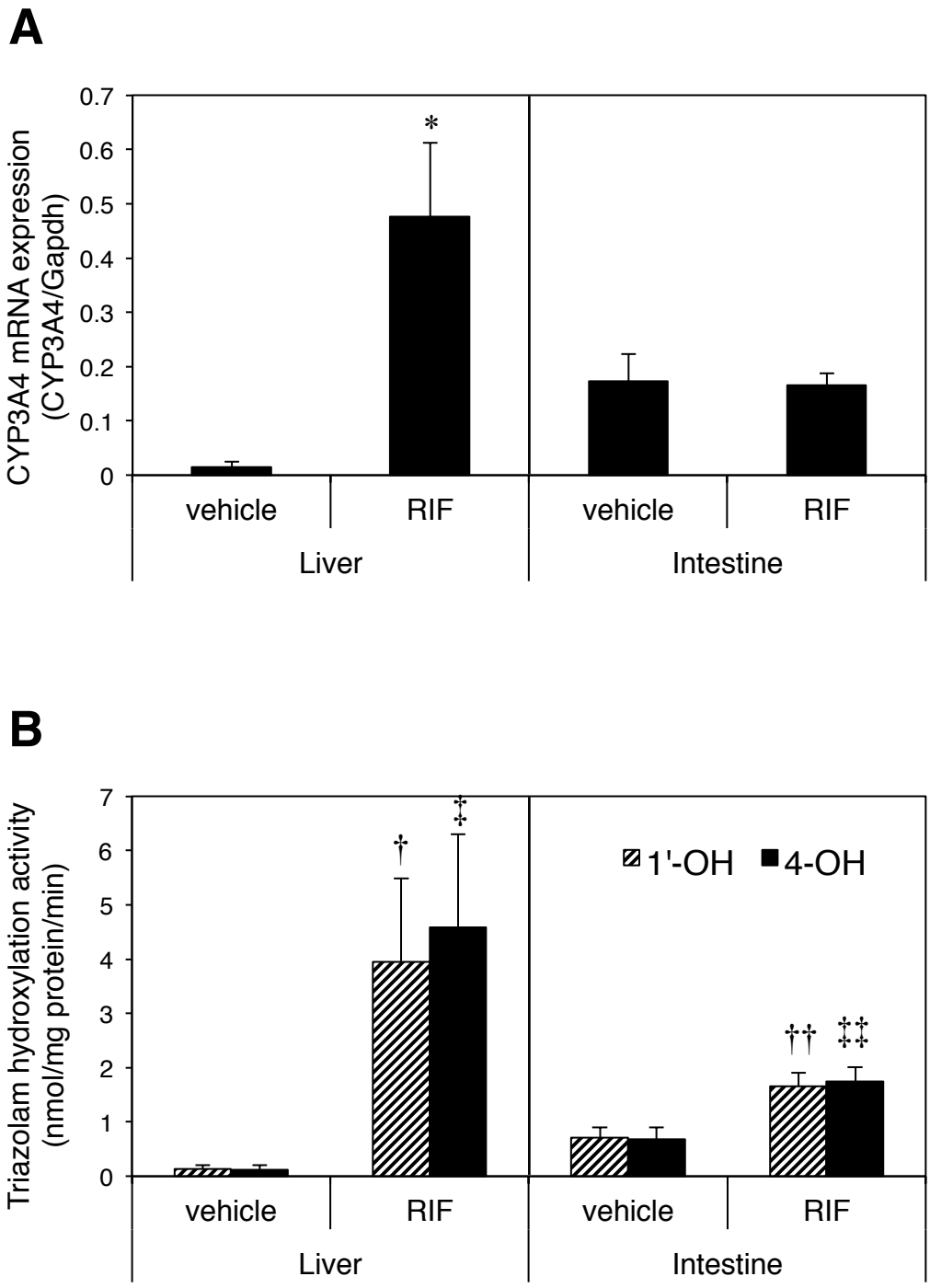

Molecular Pharmacology Fast Forward. Published on August 27, 2019 as DOI: 10.1124/mol.119.117333
This article has not been copyedited and formatted. The final version may differ from this version.

Fig. 3

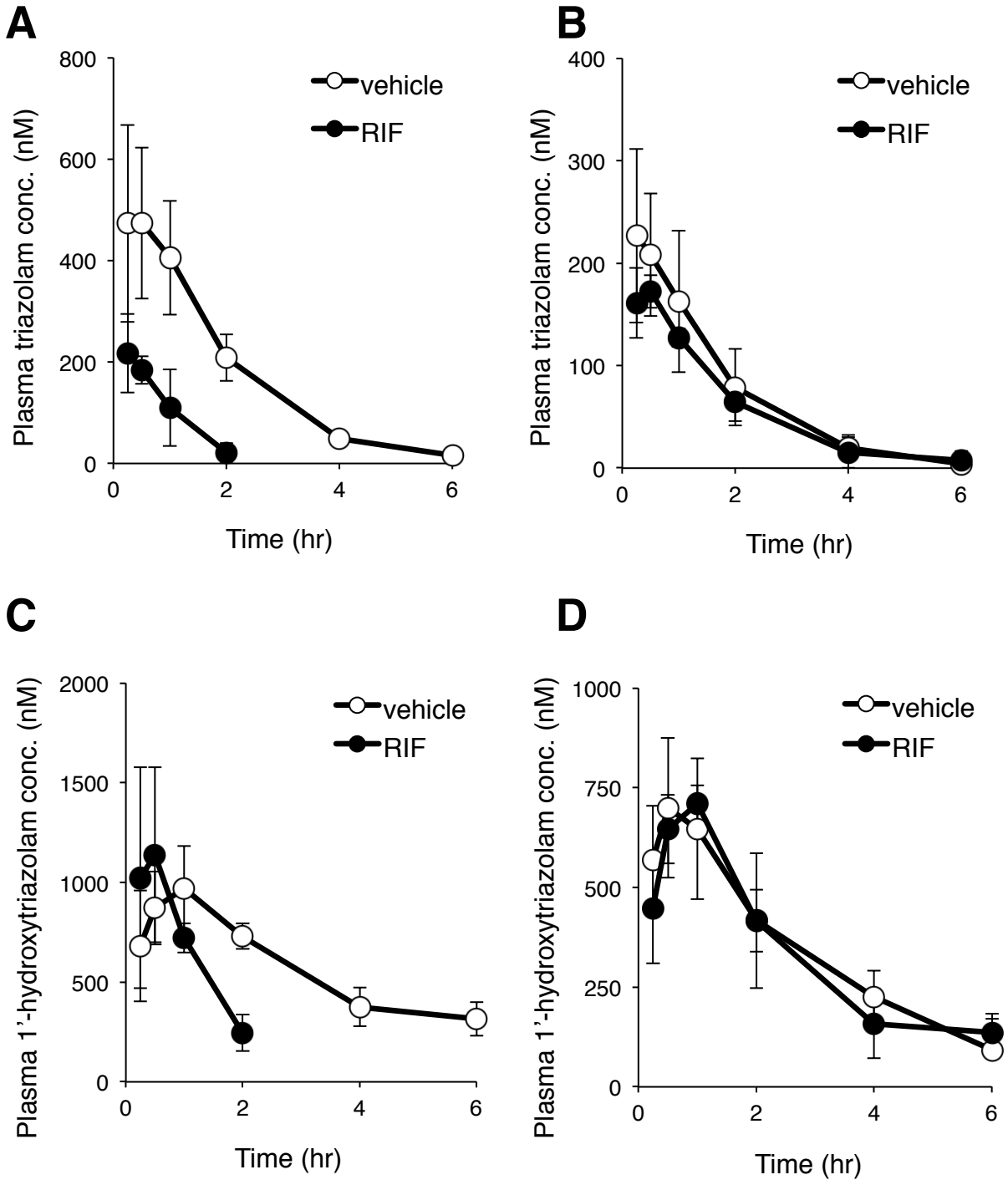

Molecular Pharmacology Fast Forward. Published on August 27, 2019 as DOI: 10.1124/mol.119.117333
This article has not been copyedited and formatted. The final version may differ from this version.

Fig. 4

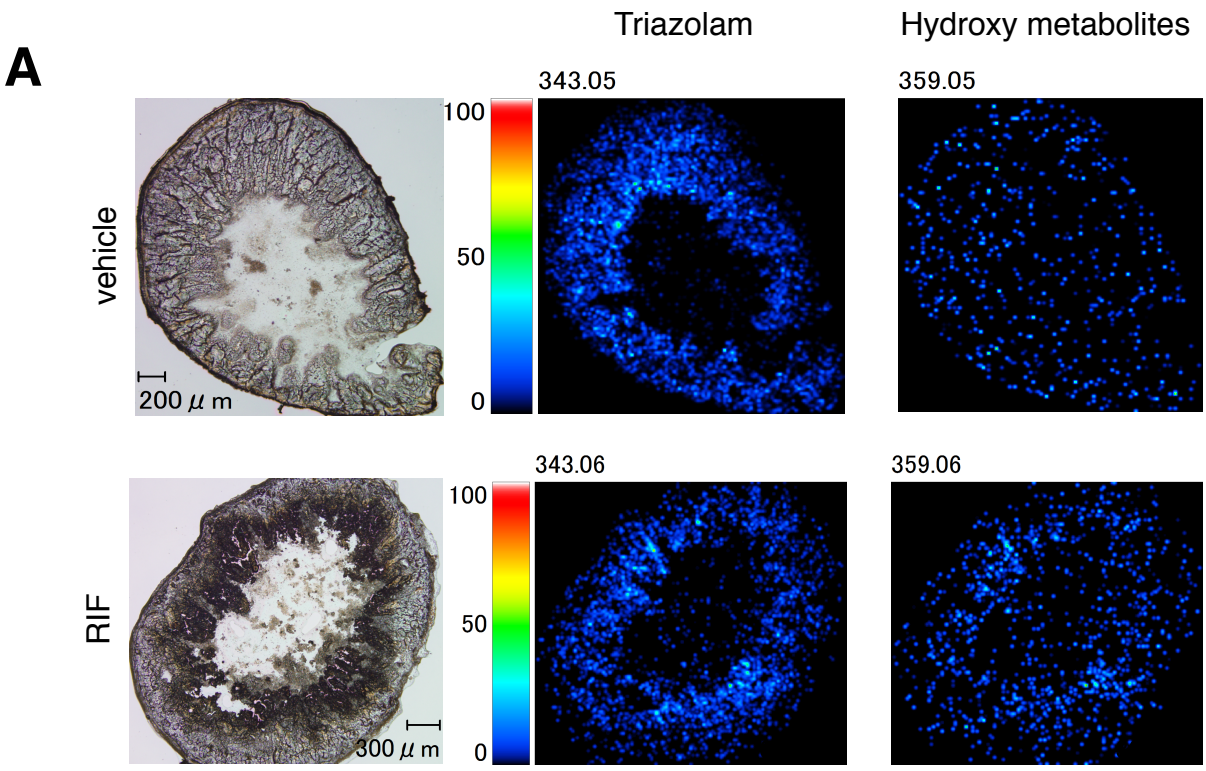

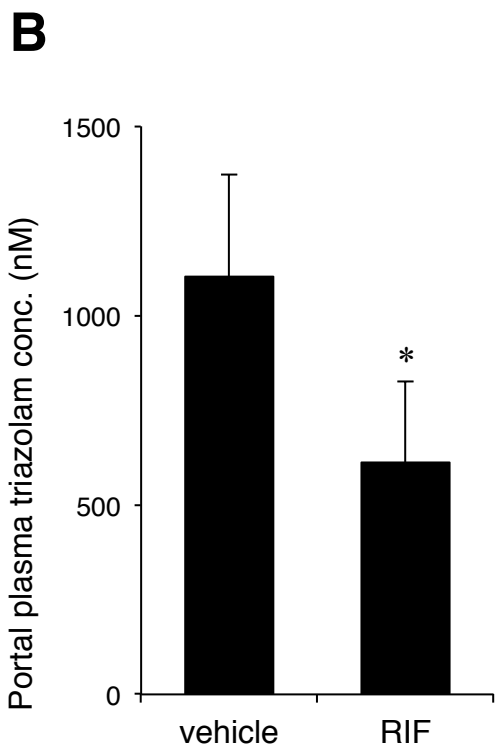

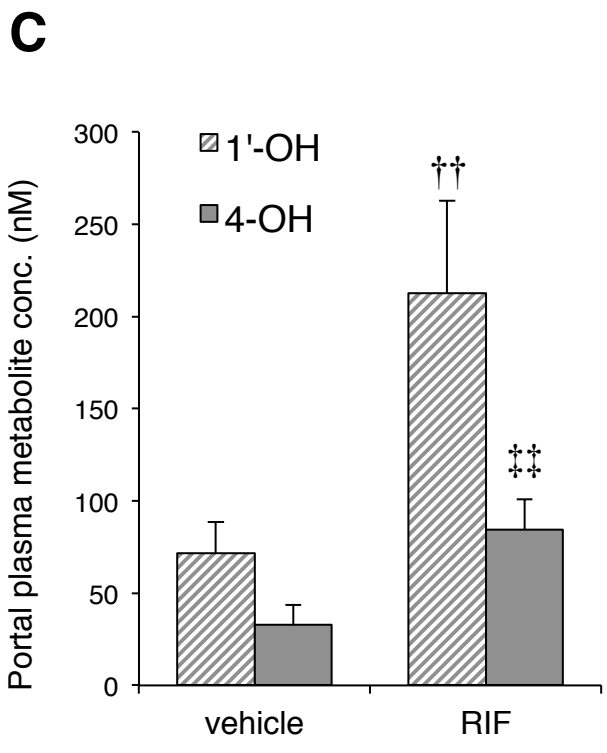

Title

CYP3A4 induction in the liver and intestine of PXR/CYP3A-humanized mice: approaches by mass spectrometry imaging and portal blood analysis

Names of Authors

Kaoru Kobayashi, Jiro Kuze, Satoshi Abe, Shoko Takehara, Genki Minegishi, Katsuhide Igarashi, Satoshi Kitajima, Jun Kanno, Takushi Yamamoto, Mitsuo Oshimura, Yasuhiro Kazuki

Journal Title

Mol Pharmacol

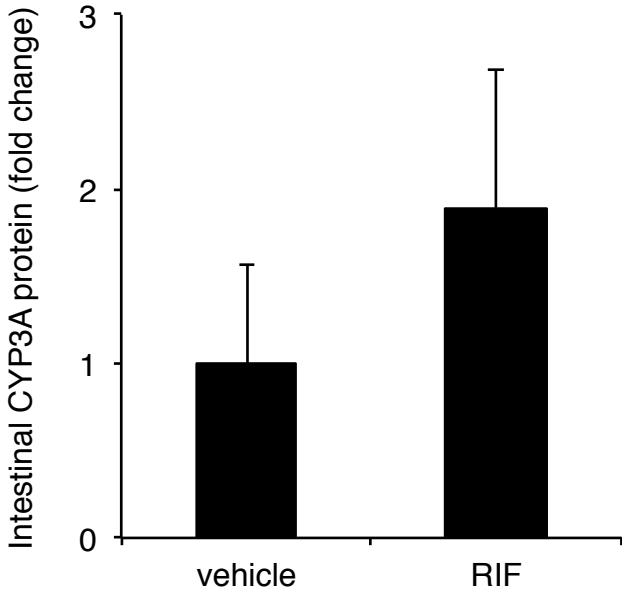

Supplemental Figure 1. CYP3A4 protein expression in intestinal microsomes of hCYP3A-MAC/hPXR mice. Mice (*N* = 4/group) were orally treated with either vehicle (0.5% CMC) or RIF (30 mg/kg) for four days. Microsomal proteins (1 μg) of small intestines were subjected to immunoblot analyses. Levels of CYP3A4 protein were normalized by those of GAPDH (loading control). The level in vehicle-treated mice was set as one. Data are expressed as means with S.D.

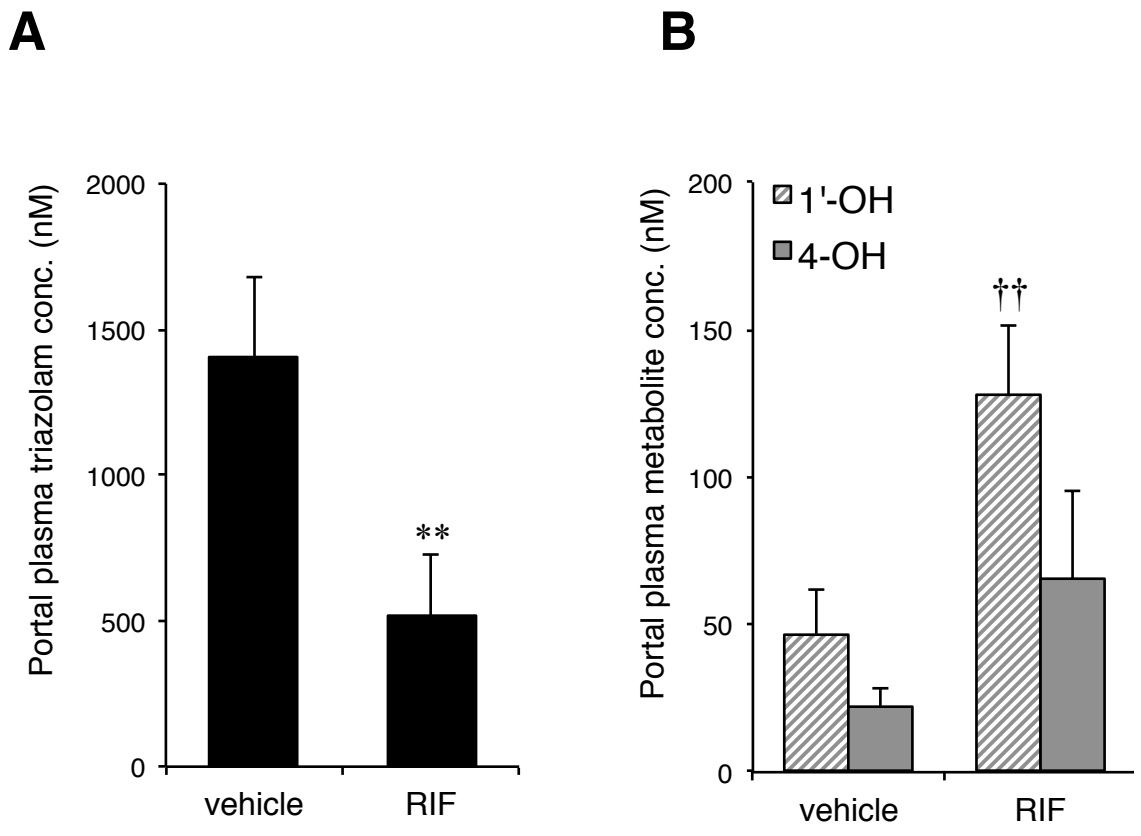

Supplemental Figure 2. Plasma concentrations of TRZ (A) and its metabolites 1'-hydroxy TRZ and 4-hydroxy TRZ (B) in the portal blood of Cyp3a-KO/hPXR mice. Mice (*N* = 4/group) were given an oral dose of the vehicle or RIF (30 mg/kg) for three days followed by 1 mg/kg oral dose of TRZ. At 10 min after TRZ dosing, blood samples were collected from portal veins. Data are expressed as means with S.D. **, $p < 0.01$ compared with a vehicle control. ††, $p < 0.01$ compared with 1'-OH of Cyp3a-KO/hPXR mice treated with a vehicle. Statistical analysis was performed with Student's *t* test.

Supplemental Table 1. Primer sequences for genomic PCR

Gene or aim	Primer name (forward)	Forward primer (5'-3')	Primer name (reverse)	Reverse primer (5'-3')
CYP3A4	CYP3A4 F7	GCAAGACTGTGAGCCAGTGA	CYP3A4 R7	GGCTGCATCAGCATCATCTA
CYP3A7	CYP3A7 F	ACCCTGAAATGAAGACGGGC	CYP3A7 R	GAGTTAATGGTGCTAACTGGGG
CYP3A5	CYP3A5 F	ATAGAAGGGTCTGTCTGGCTGG	CYP3A5 R	TCAGCTGTGTGCTGTTGTTTGC
Cyp3aKO	PGK2	TGTTCTCCTCTTCCTCATCTCC	GFP2	TGAAGGTAGTGACCAGTGTTGG
Cyp3a25	3a25 Fw	CATTGTTCTGGCTTTAGCGTC	3a25 Rv	CTGCAACCCTGAGGCTTTAG
Cyp3a13KO	neo3-1	AGTTCCAGAGGGACACCTTC	3'genome2	TTCCACACCTGGTTGCTGAC
Cyp3a13	5'down	AGATTCAAGTGGGCACACCC	3'genome2	TTCCACACCTGGTTGCTGAC
PXR KI allele	mhSXRE4	GTGAACGGACAGGGACTCAG	mhSXRSARV	CTCTCCTGGCTCATCCTCAC
PXR wt allele	WTInt5	AGTGATGGGAACCACTCCTG	WTEx6RV	TGGTCCTCAATAGGCAGGTC

Supplemental Table 2. Primer sets for the genotyping of hCYP3A-MAC, Cyp3a-KO and hPXR knock in

	Primer sets	Double humanized	WT mouse
hCYP3A-MAC (transgene)	CYP3A4 F7/R7	○	×
	CYP3A7 F/R	○	×
	CYP3A5 F/R	○	×
mouse Cyp3a knock out	PGK2/GFP2	○	×
	3a25 Fw/Rv	×	○
	neo3-1/3'genome2	○	×
	5'down/3'genome2	×	○
hPXR knock in	mhSXRE4/mhSXRSARV	○	×
	WTInt5/WTEx6RV	×	○